# Paleochronic reversion in *Psophocarpus*, the decompression function in floral anatomic fields

Edward.G.F. Benya [a, b, *] benya@unisinos.br http://www.egfbenya.com

ORCHID iD: 0000-0002-8566-8346

[a]*UNISINOS* (*Universidade do Vale do Rio dos Sinos*), *IPP (Instituto de Pesquisa de Planárias)*; visiting, where analysis was done.

[b]*Escola Agr. Sto. Afonso Rodriguez, Socopo, Cx. P. 3910, 64.051-971 Teresina, Piauí, BRAZIL*;

[b]*Quintal Botânico, Residência dos Jesuítas, 62.900-000 Russas, Ceará, (BRAZIL)* where research was done.

[*] corresponding author

phone: (55) 51 3081 4800

FAX: (55) 51 3081 4849

## Abstract

**Paleochronic reversion (an atavism) in *Psophocarpus* presents a basic floral phylloid ground state. That ground state can quickly change as permutation transformation ($T_X$) begins. The form of permutation can vary as phyllotactic phylloid ($T_{Phyld}$) and/or floral axial decompression ($T_{Axl}$) presenting linear elongation ($T_{Long}$) and/or rotational ($T_{Rtn}$) components. Research with 70 reverted floral specimens documented varying degrees of phyllotactic permutation at the bracts (Bt) region and inter-bracts (IBS) sub-region of the pre-whorls pedicel-bracts anatomic zone. Permutation further yielded an inter-zonal pericladial stalk (PCL). It continued at the floral whorls zone: the calyx (Cl), corolla (Crla), androecium (Andr), and gynoecium (Gynec) with components therein. These organ regions present a continuum as an axial dynamic vector space $\mathfrak{L}T_{Axl}$ of floral axial elongation so that anatomic sequence of permutation activity runs from the bracts (Bt) region to the carpel (Crpl) inclusive with components therein, summarized by the formula:**

$$\Sigma\, \mathbb{F}\, Bt_{(1,\ldots,z)} \pm \mathbb{S}\, IBS_{(1,\ldots,x)} \pm \Lambda\, \mathbb{F}\, PCL + \mathbb{F}\, Cl + \Lambda\, \mathbb{F}\, Corl + \Lambda\, \mathbb{F} Andr \pm \mathbb{S}\, stamen\ fltn \pm \mathbb{S}\, Andr\ spiral + \Lambda\, \mathbb{F}\, Gyncm \pm \mathbb{S}\, Gnf \pm \Lambda\, \mathbb{S}\, Cupl \pm \Lambda\, \mathbb{S}\, Crpl \pm (Crpl\ web \pm VASCARP \pm Crpl\ diadn \pm Crpl\ fltn \pm Crpl\ fltn\ no. \pm Crpl\ Rtn) = T_X.$$

**The flower reverts from a system of sexual reproductive, determinate growth to one of non-sexual, indeterminate growth.**


**Key words**: phylloid, meristem, axial elongation, demarcation event, vector space, determinate growth, indeterminate growth

Running title: **Paleochronic reversion: permutation as floral linear decompression**

## Introduction

Shoot apical meristem (SAM) genesis follows a biophysical compressed, cylindrical form whose structuring function is highly specific (Besnard et al. 2014). Classic studies have documented a "steady-state approximation for cylindrical shoot models" (Young, 1978) of the SAM whose single organ constitution, phyllotaxis and development (i.e. leaf) presents a specificity of form, at minimal variation, that is captured and summarized with precision in a single complete model (Young, 1978; Green and Baxter, 1987). The resulting compact, organ sequence of leaves presents biophysical fields as nodes and internodes whose identity is verified at bud-burst and bloom. Permutative internodal elongation ($T_{Long}$) decompression reveals phyllotactic order that, although variable, is precise (Jeune and Barabé, 2006).

That structure and exactitude change as the SAM undergoes "evocation or induction" (transformation "$T_x$") to a floral meristem (FM) whose organ composition amplifies from a single leaf morphology in the SAM to multiple organ morphologic forms of converted leaves (Battey and Lyndon, 1990; Ditta, et al. 2004; Surridge, 2004; Weigel and Meyerowitz, 1994). In most angiosperms (Stern, 1988) those converted leaves appear at two specific floral anatomic zones of pre-whorl (i.e. pedicel and bracts) and of whorls (i.e. calyx, corolla, androecium and gynoecium). The FM maintains a compact, compressed cylindrical sequence of organs, similar to the SAM, but whose exactitude of form and sequence can be affected by homeotic genes (Pautot et al. 2001; Coen and Meyerowitz, 1991; Ikeda et al. 2005; Goto et al. 2001; Honma and Goto, 2001; Kidner and Martienssen, 2005). The FM thus presents a structure similar to that of the SAM but as a reproductive system (Stern, 1988) whose organs usually distribute in biophysical fields of specific spirals and/or whorls regions (Endress and Doyle, 2007). Thus precision of the FM is less than that of the SAM. However it is still significantly specific and is summarized by a

dynamic; the ABC(DE) model (Coen and Meyerowitz, 1991; Weigel and Meyerowitz, 1994; Honma and Goto, 2001; Jack, 2004) that captures and predicts floral whorls organ identity which is also verified at bud-burst and bloom through internode elongation ($T_{long}$).

Bud decompression permutation ($T_{Long}$) (e.g. internode elongation) *in situ* (i.e. *in planta*) is crucial to both the SAM and the FM. It is minimal in the FM (a determinate growth organ system) and usually extensive in the SAM (an indeterminate growth organ system) (Parcy et al. 2002; Benya and Windisch, 2007).

The phenomenon of paleochronic reversion (i.e. an atavism) has been recognized fairly recently (Benya and Windisch, 2007). Goal of this research was to document, measure and chronicle any floral axial permutation on paleochronically reverted floral specimens originating from multiple recombinants of the species *Psophocarpus tetragonolobus* (L.) DC (fam. Fabaceae). Recombinants represented the two similar but significantly distinct environments where this reversion has been confirmed (Benya and Windisch, 2007; Benya, 2012). Analysis identified any significantly (SPSS, 2013) intense axial elongation activity at floral anatomic zones and/or regions.

**Materials and methods**

Data came from 70 paleochronically reverted floral specimens at a phylloid and/or phyllome ground state (Fig. 1 [right] and 2) originating from field-grown homeotic segregants (i.e. homozygous, recessive recombinants) (Benya, 1995) of the species *Psophocarpus tetragonolobus* (L.) DC (Fabaceae). Segregants were managed for sequential collection of floral specimens for purposes of timing analysis *in situ* or post-harvest so that “reversion age” of floral specimens served as a timing mechanism. Reversion age in days (RAD) was defined as the time from initiation of reversion (day zero) on the recombinant, to the date when any reverting floral specimen from that

recombinant entered this study. It is the time, counting from the onset of reversion on the recombinant to the date when a floral specimen entered the laboratory in a post-harvest treatment (Benya and Windisch, 2007), in accord with similar procedures (Lohmann et al. 2010). Pre-whorls and whorls anatomic zones, both juxtaposed (Fig. 1) (Besnard et al. 2014) and with phyllotactic alteration (Fig. 2 and 3) (Pinon et al., 2013) (e.g. "permutatively distanced" [Benya, 2012]) were examined and characterized for decompression longitudinal ($T_{Long}$) and/or rotational axial ($T_{Rtn}$) permutation. Permutations were qualitatively recognized by location within any of two anatomic zones (the pedicel-bracts zone and the floral whorls zone) and of five morphologic regions (fields), sub-regions (sub-fields) and active structures therein. These included bracts (Bt), calyx (Cl), corolla (Crla), androecium (Andr), gynoecium (Gynec) and components therein (e.g. gynophore and/or cupule-like structure). Quantitative count of active sites per specimen then served to measure intensity and distribution of decompression permutation.

Specimens in laboratory were divided over 33 treatments containing one to four reps per treatment primarily oriented to maintaining specimens for purposes of physical measurement and determining any age and/or timing variables influencing activity. Treatments were conducted in individual glass test-tubes and/or plastic containers in plain or deionized water within simple-structured laboratories. Humidity and temperatures within the laboratories followed closely those of external environmental conditions during the winter and spring seasons in the semi-arid, tropical equatorial climates of Teresina, Piaui, ($05^{o}05$'S; $42^{o}49$'W, alt. 64 m), from early August to late November (Gadelha de Lima, 1987) and late September to mid November in Russas, Ceará Brazil ($04^{o}55$'S; $37^{o}58$'W, alt. 20 m).

## Anatomic morphologic sequence

### Juxtaposition

Two floral anatomic zones (i.e. pre-whorl pedicel-bracts and whorls) presented six initial regions that served to begin clarifying results by anatomic location. Both zones are specific in their "normal" organs, the respective regions of those organs and the sequence(s) that define those regions. Specimens could have parallel bracts (Bt), juxtaposed to the whorls zone; calyx (Cl), corolla (Crla), androecium (Andr) and gynoecium (Gynec); juxtaposed, linearly compact (Fig. 1 [right]) reverted specimens. Categories of permutation were then based on those from published data (Benya and Windisch, 2007).

### Inter-zonal permutation

The possibility of phyllotactically altered specimens arose where floral axes were permutated presenting bracts that were physically "distanced" from the calyces by a pericladial stalk (PCL) resulting in inter-zonal longitudinal decompression (Fig. 3).

### Inter-regional permutation

A third scenario postulated decompression of specimens with bracts dislocation due to development of an inter-bracts stem (IBS) (Fig. 3) (Benya and Windisch, 2007).

Because of their recognition as defined floral whorls (Coen and Meyerowitz 1991; Parcy, et al. 1998; Schwarz-Sommer et al. 1990), each whorl is initially treated as a distinct region for possible permutation activity notwithstanding the actual permutation documented at each. Thus four additional categories of putative decompression might occur at the floral whorls zone; the sepals of the calyx, petals of the corolla, androecium and the gynoecium with its component structures especially at the carpel (Fig. 4, 5, 6) and components therein. The point of conjunction of the androecium and the gynoecium could give rise to development of a gynophore. In possible sequence with the gynophore a

cupule-like structure (Cupl) might precede the carpel (Fig. 3). The structure is termed "cupule-like" because its homology has not been confirmed. Thus six putative fields of permutation ($\mathbb{F}_{(1,\ldots,6)}$) are hypothesized herein.

**Results**

A general transformation permutation function ($T_x$) arose as webbing, vascularization, diadnation, foliation ($T_{Phyld}$) plus axial decompression ($T_{Axl}$), both longitudinal ($T_{Long}$) and/or rotational spiralling ($T_{Rtn}$). This function varied in its diversity and distribution between the two anatomic zones (ANOVA, $F_{8, 61} = 2.590$, $p = 0.017$), among the six regions within those zones ($\chi^2 = 467.732$, $p < 0.005$, d.f. = 5) and its distribution within anatomic regions (ANOVA, $F_{32, 37} = 2.831$, $p < 0.001$). Permutation usually occurred *in situ* (*in planta*). However it could continue into laboratory. Re-measurement of a sample of 25 specimens in laboratory showed a total of 7.0 mm of PCL and/or IBS development among two specimens; one mm of PCL and six of IBS, statistically not significant ($\chi^2 = 0.0144$, NS, d.f. = 1). Thus decompression *in situ* (immediate post-harvest) was taken as the overall measure of permutation in accord with similar procedures (Piao *et al.* 2015).

Loci of the bracts anatomically defined the bracts region which extended from zero (i.e. bracts parallel or normal) (Fig. 2) to 12 mm depending on dislocation and development of any IBS (Fig. 3). This occurred on 31 specimens. Inter-zonal decompression yielded a PCL which developed in lengths of one to 38 mm on 60 specimens. This was usually accompanied (but at times preceded or succeeded) by formation of an IBS. One or both of these then constituted the "Axial active" ($n = 63 \sum = 808.0$ mm) measure of permutation activity on most specimens. PCL and IBS dislocations were distinct. Each could occur separately (i.e. three IBS and 32 PCL) on

different specimens or concurrently on 28 specimens. Gynophore and/or cupule-like structural development occurred on 27 specimens.

The sum of the lengths of the IBS and PCL (i.e. “Axial active” elongation) plus those of the gynophore and cupule-like structure formed the “Axial complete” measure (n = 65 $\sum$ = 1095.0 mm) of “longitudinal decompression”. “Axial active” was the principal, significant ($F_{32,37}$ = 6.947, $p < 0.000$) component (73.79%) of “Axial complete” decompression whose length was more specifically constituted by PCL lengths ($F_{31,28}$ = 3.791, $p < 0.000$). Linear axial displacement of a locus or loci in an established direction or directions (i.e. along the floral axis) at these four sites defined the principal demarcation components of longitudinal ($T_{Long}$) permutation (126 of 274 sites) where each “demarcation event is a vector” (Green & Baxter 1987). A spiral ($T_{Rtn}$) displacement of carpel sites of the gynaecium arose (n = 6 specimens), a distinct topological dislocation vector function and thus not part of floral axial longitudinal displacement function.

Regional decompression on two of the seven juxtaposed bracts-calyx specimens presented cupule-like structures. Thus the final ratio of confirmed axial decompression permutation to non-axial decompression specimens was 65:5.

Overall permutation activity was significantly more intense within the whorls zone (183 sites) than within the pre-whorls zone (91 sites) ($t = 2.335$, $p = 0.022$, $df = 69$). This significance continued within both climatic regions. Research then focused on anatomic regions within both zones, the intensity and possible sequence(s) of decompression within and between regions, plus any distinctions in decompression between the two significantly different environments (Benya, 2012). “Axial complete” measure at 1095 mm of longitudinal floral decompression occurred over 2421 “reversion age in days” (RAD) at a mean value of 0.452 mm per RAD with a range of 0.003 to 3.563 mm per RAD.

The difference between the 126 decompression sites and the 148 general permutation sites was not significant ($\chi^2 = 1.7664$, NS, d.f. = 1). Timing of both decompression and general permutation functions at the gynoecium was significant across and within both environments ($F_{24, 39} = 2.791$, $p < 0.002$). Significance continued in the diversity of sites and events ($F_{24, 39} = 3.097$, $p < 0.000$) at and within the carpel; at the gynophore and cupula-like structure. This included webbing between carpel clefts, vascularization, diadnation, foliation, spiralling, putative ovule permutation (also as vascularization, elongation, and/or foliation) in sequence and/or combination with some or all of these antecedent functions, across and within both environments. This reflected the complexity of structure of the carpel and the diversity of activity that could occur at that sub-region (Benya, 2012, Trigueros et al. 2009).

Parallel non-webbed carpel clefts at both environments preceded any permutation function at the carpel and probably preceded permutation at any other anatomic region. This is the "ground state" of the carpel. Permutative decompression of the carpel begins with webbing between carpel clefts (Fig. 4) and/or spiralling (Fig. 3). Both webbing and spiralling were virtually impossible to time through RAD in either environment as both were *in situ* functions and usually preceded *in planta* flower bloom thus impeding simple empirical verification. They were, however confirmed as "initiating functions" by means of dissection of pre-bloom flowers (i.e. flower buds) whose further permutation activity was thus eliminated because of dissection.

Amplification at the calyces (n = 8) ($t = -14.049$, $p < 0.000$, df = 69), foliation of petals at the corolla (n = 2) ($t = -31.104$, $p < 0.000$, df = 69) (Fig. 2), plus foliation of the anther (n = 2) ($t = -31.104$, $p < 0.000$, df = 69) at the androecium all arose at low levels ($T_{Phyld}$). Gynophore development was minimal in both environments (n = 8) ($t = -8.765$, $p < 0.000$, df = 69). Cupule-like structure development followed a norm (n = 27) (t = –

1.097, p = 0.276, df = 69) commensurate with decompression at the IBS (n = 31) (t= – 0.119, p = 0.905, df = 69). However it showed significant negative correlation (r= – 0.384; p < 0.002) with RAD because it arose early in the decompression sequence.

Permutation as decompression and vascularization followed (*in situ*) a sequence whose origin from the ground state carpel was apparently in putative invariable unbroken steps. These could terminate at any step as: un-webbed to webbed, then perhaps to vascularized, then at times to diadnation, then sometimes to foliation (Fig. 6) (Table 1).

Two general sequences of permutation activity are manifest in this data. The first sequence involves metric intensity of activity between anatomic zones, regions and sub-regions beginning at the bract-calyx juncture. Overall intensity of site activity (n = 274) followed a significant cubic regression on axial complete decompression (1095 mm) (cubic $r^2 = 0.288$, $F_{3,66} = 8.890$, p □ 0.000**)** from bracts to whorls inclusive. That regression continued for the four floral whorls themselves (n = 183 sites) (cubic $r^2 = 0.237$, $F_{3,66} = 6.844$, p □ 0.000), into the fourth whorl gynaecium (n = 171 sites) (cubic $r^2 = 0.204$, $F_{3,66} = 5.653$, p □ 0.002) and total carpel structures (n = 136) (cubic $r^2 = 0.111$, $F_{3,66} = 2.747$, p □ 0.050). Webbing (40 specimens), vascularization (38 specimens), diadnation (27 specimens) carpel foliation (25 specimens), and internal carpel foliation number (n = 61) (cubic $r^2 = 0.121$, $F_{3,66} = 3.024$, p □ 0.036) continued this sequence of significant cubically varying intensity. Spiralling, not a necessary function of the carpel sequence, occurred at a non-significant level (cubic $r^2 = 0.049$, $F_{3,66} = 1.131$, p = 0.343) (six specimens) and only at Russas.

A second sequence involved timing. This placed webbing of the carpel (usually in Teresina) and/or spiralling of the carpel (usually in Russas) as initiatory or co-initiatory events closely followed by minimal but early calyx amplification on the pre-bloom flower. Diadnation and foliation of the carpel could then follow webbing in as little as 24

hours. Where carpel vascularization occurred, it preceded diadnation and foliation of the carpel. However this depended on weather and climatic conditions (Benya, 1995, 2012). Gynophore and/or cupule-like structural formation might follow webbing.

IBS and/or PCL formation in relation to RAD was significant (ANOVA $F_{24,39}$ = 2.109, p = 0.019). That formation could be almost initiatory, but its significantly broad physically spatial distribution as a component of Axial complete length; 808 of 1095 mm (ANOVA $F_{32,37}$ = 6.947, p < 0.000) rank it among the most time consuming of events in relation to RAD (r = 0.196; p = 0.121, n = 64).

As in the case of site analysis in relation to axial metric decompression, regression analysis revealed dynamics of site establishment in relation to RAD of specimens. Overall intensity of site activity (n = 274 sites) showed linear but not significant response to RAD. However whorls site activity (n = 183) did present significant quadratic (curvilinear) response to RAD ($r^2$ = 0.107, $F_{2,61}$ = 3.670, p < 0.031), as did site activity at the gynaecium (n = 171) ($r^2$ = 0.103, $F_{2,61}$ = 3.518, p < 0.036). It remained as such for structures internal to the carpel (n = 136) ($r^2$ = 0.150, $F_{2,61}$ = 5.392, p < 0.007) and even carpel spiralling (n = 6 sites) ($r^2$ = 0.214, $F_{2,61}$ = 8.282, p = 0.001).

## Discussion

A phylloid ground state and/or various degrees of phyllome organ formation (Pelaz et al., 2000; Weigel and Meyerowitz, 1994) characterized all 70 experimental specimens. Floral meristem cancellation (Benya and Windisch, 2007), was anticipatory and essential to that phylloid state. After that, most specimens entered into a permutation phase of transformation ($T_x$) that could include organ foliation ($T_{Phyld}$) (Fig. 2) and/or a decompression function ($T_{Axl}$) of the floral axis, itself constituted by axial elongation ($T_{Long}$) and/or a rotational dynamic of axial spiral (Okabe 2011, 2015) permutation ($T_{Rtn}$).

The permutation function was significant *in situ* (*in planta*) but could extend to post-harvest. By deduction, it usually began in the carpel of the gynoecium as webbing between carpel clefts and/or rotational spiralling of the carpel. This was usually prior to flower bloom, thus specific (*in vivo*) timing of these two events was impossible.

Bracts regions usually entered a morphologically active phase of elongation (Pinon et al., 2013; Besnard et al., 2014; Bargmann et al., 2013; Benya and Windisch, 2007). These were the most striking in their manifestations of the permutation elongation phase as IBS and/or PCL. However decompression as gynophore and/or cupule-like structure formation contributed to overall axial elongation. Rare yet at times solitary presence of PCL, IBS and cupule-like structures indicated that a distinct vector governs each of these decompression events. Those distinctions coincide with Mendelian proportions indicating dominant:recessive genetic functions underlying IBS and PCl presence or absence (Benya and Windisch, 2007; Benya, 2012) . Specific governance at the gynophore cannot be determined from this data.

Bracts (with any IBS therein) plus any PCL show continuity to the calyces presenting a succession of distinct fields and sub-fields ($\mathbb{F}$ Bt $\pm$ $\mathbb{S}$ IBS $\pm$ $\bigwedge$ $\mathbb{F}$ PCL + $\bigwedge$ $\mathbb{F}$ Cl) representing temporal and physically spatial activity. The PCL is a biophysical field ($\mathbb{F}$ PCL) whose varying morphologic length, specific for each specimen, serves to distance the Cl field ($\mathbb{F}$ Cl) and Bt field ($\mathbb{F}$ Bt) from each other. The anatomic regions ($\mathbb{F}$ $Bt_{(1,\ldots,z)}$ $\pm$ $\mathbb{S}$ $IBS_{(1,\ldots,x)}$ $\pm$ $\bigwedge$ $\mathbb{F}$ PCL $\pm$ $\mathbb{F}$ Cl $\pm$ …$\bigwedge$ $\mathbb{F}$ Gyncm) constitute the permutated floral axis (Axl), beginning at Bt regions and extending to the carpel (Crpl) of the gynoecium inclusive; a continuum of structure that is a dynamic longitudinal linear axial vector space $\mathfrak{L}T_{Axl}$.

Besides distancing bracts from calyces, a PCL also distanced the entirety of the floral pre-whorls anatomic zone ($\mathbb{F}$ $Bt_{(1,\ldots,z)}$ $\pm$ $\mathbb{S}$ $IBS_{(1,\ldots,x)}$) from the whorls anatomic zone ($\mathbb{F}$ Cl+ ... +$\mathbb{F}$ Gyncm). Results indicate definite regional homeostatic canalization

associated with paleochronic floral reversion (Benya and Windisch, 2007). Canalization continued to be manifest as floral permutation up to and including axial elongation at these anatomic zones and their respective organs regions (Okamuro et al., 1993).

Lack of any significant correlation between RAD and permutation activity at the calyces, corollas and androecium reflects their robust phenotypes resulting from canalization of organ identities (Debat and David, 2001; Okamuro et al. 1993) and resulting stability at these regions. Intensity of activity diminished between the calyx (eight specimens) and gynophore (eight specimens) to a minimum at the corolla and androecium (two specimens each). It then increased from eight at the gynophore to 26 specimens with a cupule-like structure and then to the 63 specimens with a total of 136 carpel permutation sites. Cubic regression thus reflected the inversely varying robusticity of organ identity (due to canalization) with permutation function from pre-whorls into whorls floral sites. Presence but lack of any significant relation of the spiralling function (n = 6) with overall permutation site genesis (n = 274) reflects the distinction between whorls genesis and the spiralling function (Okabe, 2011).

Juxtaposition of floral anatomic zones and organs regions is the phyllotactic norm for this and most other angiosperm species. During elongation, floral organs maintain their specified identities at definite positions of their respective loci (Benya and Windisch, 2007). However expansion of anatomic organ regions, by means of PCL, IBS, gynophore, etc. can augment organ regional longitudinal dimensions and even change locus orientation and fields.

## Conclusion

Sexually reproductive flowers can revert (transmutation) from the determinate growth reproductive state to a non-reproductive phylloid state. Reverted flowers can then

enter a permutation phase where elongation spacing of organ regions occurs along the floral axis. Distinct biophysical functions affect that permutation phase.

Spiralling function in the SAM can be captured with mathematical precision (Okabe, 2011) while overall SAM genesis can be captured in a simple model (Young, 1978). That model can be expanded in the FM to a distinct ABC(DE) model of homeotic gene function for floral whorl genesis. Cancellation of the dynamic of the ABC(DE) model leads to a floral ground state. A permutation function can then arise. The permutation functions documented here manifest significant and variable presence in a significantly specific but variable timing sequence as reverted flowers demonstrate a return to indeterminate growth in this "Axial permutation" model. This model contains both axial decompression and foliation components ($T_X = T_{Axl} + T_{Phyld}$), the prior of which is composed of axial longitudinal ($T_{Long}$) and axial spiral ($T_{Rtn}$) components so that:

$T_{Axl} = T_{Long} + T_{Rtn}$, where:

$T_X = (T_{Long} + T_{Rtn}) \subset T_{Axl} + T_{Phyld}$

Variability of the ABC(DE) model is due to variable activity of homeotic genes. Variability of this "Axial permutation model" is also due to homeotic genes (Benya and Windisch, 2007) but their activation is significantly correlated with climatic and weather factors (Benya 2012). Resulting anatomic sequence of permutation activity then runs from the bracts (Bt) region to the carpel inclusive with components therein. The formula:

$$\mathbf{\Sigma\, \mathbb{F}\, Bt_{(1,\ldots,z)} \pm \mathbb{S}\, IBS_{(1,\ldots,x)} \pm \Lambda\, \mathbb{F}\, PCL + \mathbb{F}\, Cl + \Lambda\, \mathbb{F}\, Corl + \Lambda\, \mathbb{F}\, Andr \pm \mathbb{S}\, stamen\ fltn \pm \mathbb{S}\, Andr\ spiral + \Lambda\, \mathbb{F}\, Gyncm \pm \mathbb{S}\, Gnf \pm \Lambda\, \mathbb{S}\, Cupl \pm \Lambda\, \mathbb{S}\, Crpl \pm (Crpl\ web \pm VASCARP \pm Crpl\ diadn \pm Crpl\ fltn \pm Crpl\ fltn\ no. \pm Crpl\ Rtn) = T_X}$$ (Supplementary Material).

summarizes the complete anatomic sequence of permutation transformation ($T_X$) in its phylloid ($T_{Phyld}$) and floral axial decompression ($T_{Axl}$) aspects with linear elongation ($T_{Long}$) and/or rotational ($T_{Rtn}$) constituents. The principal components of the longitudinal axial

vector space ($T_{Long}$) within the "Axial permutation model" ($T_{Axl}$) are captured by the formula:

$$\mathbb{F}\ Bt_{(1,\ldots,z)} \pm \mathbb{S}\ IBS_{(1,\ldots,x)} \pm \bigwedge \mathbb{F}\ PCL\ldots \pm \bigwedge \mathbb{S}\ Gnf \pm \bigwedge \mathbb{S}\ Cupl \approx T_{Long} \in T_{Axl}\ \text{as}\ \mathfrak{L}T_{Long}$$

Biophysical functions affect the permutative phase at the anatomic and morphologic regions studied here. A continuum might extend to further morphologic fields generated on flowers of species whose bract numbers increase in multiples beyond the dual-bract flower structure addressed herein. Theoretically that continuum could be extended longitudinally in segments of varying lengths defined by each bract in a flower of multi-bract species (e.g. *Euphorbia pulcherrima*, *Cornus florida*, *Quercus* sp.) whenever the master "*srs*" recessive allele (Benya and Windisch, 2007), homozygous and activated, is accompanied by the necessary "reversion dependent genes" (Benya, 2012; Benya and Windisch, 2007). Each bract would thus define a specific field ($\mathbb{F}\ Bt_{(1,\ldots,z)}$) with possible accompanying sub-fields of IBS ($\mathbb{S}\ IBS_{(1,\ldots,x)}$) with any PCL ($\mathbb{F}\ PCL$) as part of the overall formula from bracts to carpel $\overline{Bt, Crpl} = T_X$ in anatomic sequence constituting a dynamic vector space $\mathfrak{L}T_{Axl}$ whose presence on living specimens of extant species offers a unique tool for research.

**Acknowledgements**

Saint John's College, Landivar, Belize City, Belize, (T. Thompson, professor) provided an introduction to material. G.R. Lovell (Griffin, Gerogia, USA), W. Denny (Beltsville, Maryland, USA) USDA-ARS, T.N. Khan, Dept. Agr. Western Australia and H.P.N. Gunasena, U. Peradeniya, Sri Lanka provided seed. A.C. Machin assisted with seed importation. Escola Agrícola Santo Afonso Rodriguez, (J. Moura Carvalho, E.M. Moreira, J. Bulfoni and I. Govoni) and Escola Técnica Soinho provided facilities for experimentation. The “Universidade do Vale do Rio dos Sinos” (UNISINOS) and “Laboratório de Histologia” (Ana Leal-Zanchet, coordinator) furnished facilities for analysis. A. DePaula, J. M. daSilva, E.O. Alves, J. deFreitas, C.G. deOliveira, F. Gil and G. & H. Galik helped with technical work and analysis. P G. Windisch, M.C. Moura Carvalho, C. Radz, S.J.V. Benya and T. H. Oliveir assisted with manuscript preparation.

**Compliance with ethical standards**

**Conflict of interest:** The author declares that he has no conflict of interest.

## REFERENCES

Bargmann, B. O. R., Vanneste, S., Krouk, G., Nawy, T., Efroni, I., Shani, E., Choe, G., Friml, J., Bergmann, D. C., Estelle, M. and Birnbaum, K. D. (2013): A map of cell type-specific auxin responses. - *Molec. Sys. Bio*. **9: 688 - 700. doi: 10.1038/msb.2013.40**

Battey, N. H. and Lyndon, R. F. (1990): Reversion of flowering. - *Bot Rev.* **56: 162 - 189**. http://dx.doi.org/10.1007/BF02858534

Benya, E. G. F. (1995): Genetic aspects of flower reversion in the winged bean [*Psophocarpus tetragonolobus* (L.) DC]. - *Acta Biol. Leopoldensia* **17: 65 - 72**.

Benya, E. G. F. (2012): Permutation of ground state phylloid buds and flowers from a paleobotanically reverted recombinant of *Psophocarpus*. - *Res. & Rev in Biosci* **6: 221 - 230**. **ORCHID iD: 0000-0002-8566-8346**

Benya, E. G. F. and Windisch, P. G. (2007): A phylloid ground state of reverted floral specimens of *Psophocarpus tetragonolobus* (L.) DC (Fabaceae): cancelled floral meristem and continued floral organ identity. - **Flora 202: 437 - 446**. doi:10.1016/j.flora.2006.09.004

Besnard, F., Refahi, Y., Morin, V., Marteaux, B., Brunoid, G., Chambrier, P., Rozier, F., Mirabet, V., Legrand, J., Laine, S., Thévenon, E., Farcot, E., Cellier, C., Das, P., Bishopp, A., Dumas, R., Parcy, F., Helariutta, Y., Boudaoud, A., Godin, C., Traas, J., Guédon, Y. and Vernoux, T. (2014): Cytokinin signaling inhibitory fields provide robustness of phyllotaxis. *Nature* **505: 417 - 421**. doi:10.1038/nature12791

Coen, E. S. and Meyerowitz, E. M. (1991): The war of the whorls: genetic interactions controlling flower development. *Nature* **353: 31 - 37**. doi:10.1038/353031a0

Debat, V. and David, P. (2001): Mapping phenotypes: canalization, plasticity and developmental stability. *Trends Ecol Evol* **16:555 - 561**. doi:10.1016/S0169-5347(01)02266-2

Ditta, G., Pinyopich, A., Robles, P., Pelaz, S. and Yanofsky, M. F. (2004): The *SEP4* gene of *Arabidopsis thaliana* functions in floral organ and meristem identity. *Curr. Biol*. **14: 1935 - 1940**. doi:10.1016/j.cub.2004.10.028.

Endress, P. K. and Doyle, J. A. (2007): Floral phyllotaxis in basal angiosperms: development and evolution. *Curr. Opin. Plant Biol.* **10: 52 - 57**. doi 10.1016/j.pbi.2006.11.007

Gadelha de Lima, M. (1987): *O Clima de Teresina, Teresina*. Fundação Universidade Federal do Piauí, Teresina, 8 pp.

Goto, K., Kyozuka, J. and Bowman, J. L. (2001): Turning floral organs into leaves, leaves into floral organs. *Curr. Opin. Genet. Dev.* **11: 449 - 456**. http://dx.doi.org/10.1016/S0959-437X(00)00216-1

Green, P. B. and Baxter, D. R. (1987): Phyllotactic patterns: characterization by geometrical activity at the formative region. *J. Theor. Biol.* **128: 387 - 395**. doi: 10.1016/S0022-5193(87)80080-2

Honma, T. and Goto, K. (2001): Complexes of MADS-box proteins are sufficient to convert leaves into floral organs. *Nature* **409: 525 - 529**. doi:10.1038/35054083

Ikeda, K., Nagasawa, N. and Nagato, Y. (2005): *ABERRANT PANICLE ORGANIZATION 1* temporarily regulates meristem identity in rice. *Dev Biol*. **282: 349 - 360**. doi:10.1016/j.ydbio.2005.03.016

Jack, T. (2004): Molecular and genetic mechanisms of floral control. *Plant Cell* **16: (supplement) S1 - S17**. doi:10.1105/tpc.017038

Jeune, B. and Barabé, D. (2006): A stochastic approach to phyllotactic patterns analysis. *J Theor Biol* **238: 52 - 59**. doi:10.1016/j.jtbi.2005.05.036

Kidner, C. A. and Martienssen, R. A. (2005): The role of ARGONAUTE1 (AGO1) in meristem formation and identity. *Dev Biol*. **280 (2): 504 - 517**. doi:10.1016/j.ydbio.2005.01.031.

Lohmann, D., Stacey, N., Breuninger, H., Jikumaru, Y., Müller, D., Sicard, A., Leyser, O., Yamaguchi, S. and Lenhard, M. (2010): SLOW MOTION is required for within-plant auxin homeostasis and normal timing of lateral organ initiation at the shoot meristem in *Arabidopsis*. *Plant Cell*. **22: 335 - 348**. doi:10.1105/tpc.109.071498

Okabe, T. (2011): Physical phenomenology of phyllotaxis. *J Theor Biol* **280: 63 - 75**. doi: 10.1016/j.jtbi.2011.03.037

Okabe, T. (2015): Biophysical optimality of the golden angle in phyllotaxis. *Sci. Rep* **5: 15358**. doi: 10.1038/srep15358

Okamuro, J. K., denBoer B. G. W. and Jofuku, K.D. (1993): Regulation of Arabidopsis flower development. *Plant Cell* **5: 1183 - 1193**. doi:10.1105/tpc.5.10.1183

Parcy, F., Nilsson, O., Busch. M. A., Lee, I. and Weigel, D. (1998): A genetic framework for floral patterning. *Nature* **395: 561 - 566**. doi:10.1038/26903

Parcy, F., Bomblies, K. and Weigel, D. (2002): Interaction of *LEAFY, AGAMOUS* and *TERMINAL FLOWER1* in maintaining floral meristem identity in *Arabidopsis*. *Development* **129: 2519 - 2527**.

Pautot, V., Dockx, J., Hamant, O., Kronenberger, J., Grandjean, O., Jublot, D. ans Traas, J. (2001): *KNAT2*: Evidence for a link between knotted-like genes and carpel development. *Plant Cell* **13: 1719 - 1734**. doi:10.1105/TPC.010184

Pelaz, S., Ditta, G. S., Baumann, E., Wisman, E. and Yanofsky, M. F. (2000): B and C floral organ identity functions require *SEPALLATA* MADS-box genes. *Nature* **405: 200 - 203**. doi:10.1038/35012103

Piao, S., Tan, J., Chen, A., Fu, Y. H., Ciais, P., Liu, Q., Janssens, I. A, Vicca, S., Zeng, Z., Jeong, S.-J., Li, Y., Myneni, R. B., Peng, S., Shen, M. and Peñuelas, J. (2015): Leaf onset in the northern hemisphere triggered by daytime temperature. *Nat Comm* **6: 6911**. doi:10.1038/ncomms7911

Pinon, V., Prasad, K., Grigg, S. P., Sanchez-Perez, G. F. and Scheres, B. (2013): Local auxin biosynthesis regulation by PLETHORA transcription factors controls phyllotaxis in *Arabidopsis*. *Proc. Natl. Acad. Sci. USA* **110: 1107 - 1112**. doi:10.1073/pnas.1213497110

Schwarz-Sommer, Z., Huijser, P., Nacken, W., Saedler, H. and Sommer, H. (1990): Genetic control of flower development by homeotic genes in *Antirrhinum majus*. *Science* **250: 931 - 936** doi: 10.1126/science.250.4983.931

Stern, K. R. (1988): *Introductory Plant Biology*. 4th edn. Wm. C. Brown Publishers, Dubuque, 616 pp.

Surridge, C. (2004): Plant development: A bunch of leaves. *Nature* **432: 161** doi:10.1038/432161a

Trigueros, M., Navarrete-Gómez, M., Sato, S., Christensen, S. K., Pelaz, S., Weigel, D., Yanofsky, M. F. and Ferrándiz, C. (2009): The NGATHA genes direct Style development in the *Arabidopsis* gynoecium. *Plant Cell* **21: 1394 - 1409**. doi:10.1105/tpc.109.0655508

Weigel, D. and Meyerowitz, E. M. (1994): The ABCs of floral homeotic genes. *Cell* **78: 203 - 209**. doi:10.1016/0092-8674(94)90291-7

Young, D. A. (1978): On the diffusion theory of phyllotaxis. *J. Theo. Biol* **71: 421 - 432**.

doi:10.1016/0022-5193(78)90169-8

**FIGURES (Captions)**

**Figure 1**. Flowers *Psophocarpus tetragonolobus*; normal (i.e. wild type; [left]) and reverted (i.e. a phylloid state, meristematically inactive, bracts and calyx regions juxtaposed; [right]).

**Figure 2**. Reverted flower presenting beginning phyllome condition of whorls organs and permutation:

carpel (top)

petals (ptl) [sides]

stamens (normal) [stamens region]

calyx region [sepals]

pericladial stalk (PCL)

bracts (parallel) and calyx regions distanced about 1 cm from each other.

**Figure 3**. Bracts (Bt) and bracts dislocation forming an “inter-bracts stem” (IBS) of about 4 mm (measured from locus centre of one bract to locus centre of second bract); Pericladial stalk (PCL) of about 8 mm distancing pedicel-bract zone from whorls zone; Calyx (petals and stamens removed for clarity); Gynophore (Gnf) of about 12 mm connecting to a Cupule-like structure (Cupl) of about 8 mm leading to a webbed carpel (Crpl) showing vascularization and initial spiralling.

**Figure 4.** Webbing between carpel clefts is the first necessary step in permutation at the carpel.

**Figure 5**. Vascularized carpel with initial diadnation of about 60%, acropetal along adaxial cleft.

**Figure 6**. Permutated carpel on extended cupule-like structure presenting the four necessary permutation steps leading to complete carpel foliation:

1. Webbing between carpel clefts;
2. Vascularized webbing
3. Carpel diadnation (acropetal along adaxial cleft);
4. Initial carpel foliation (putative ovules).

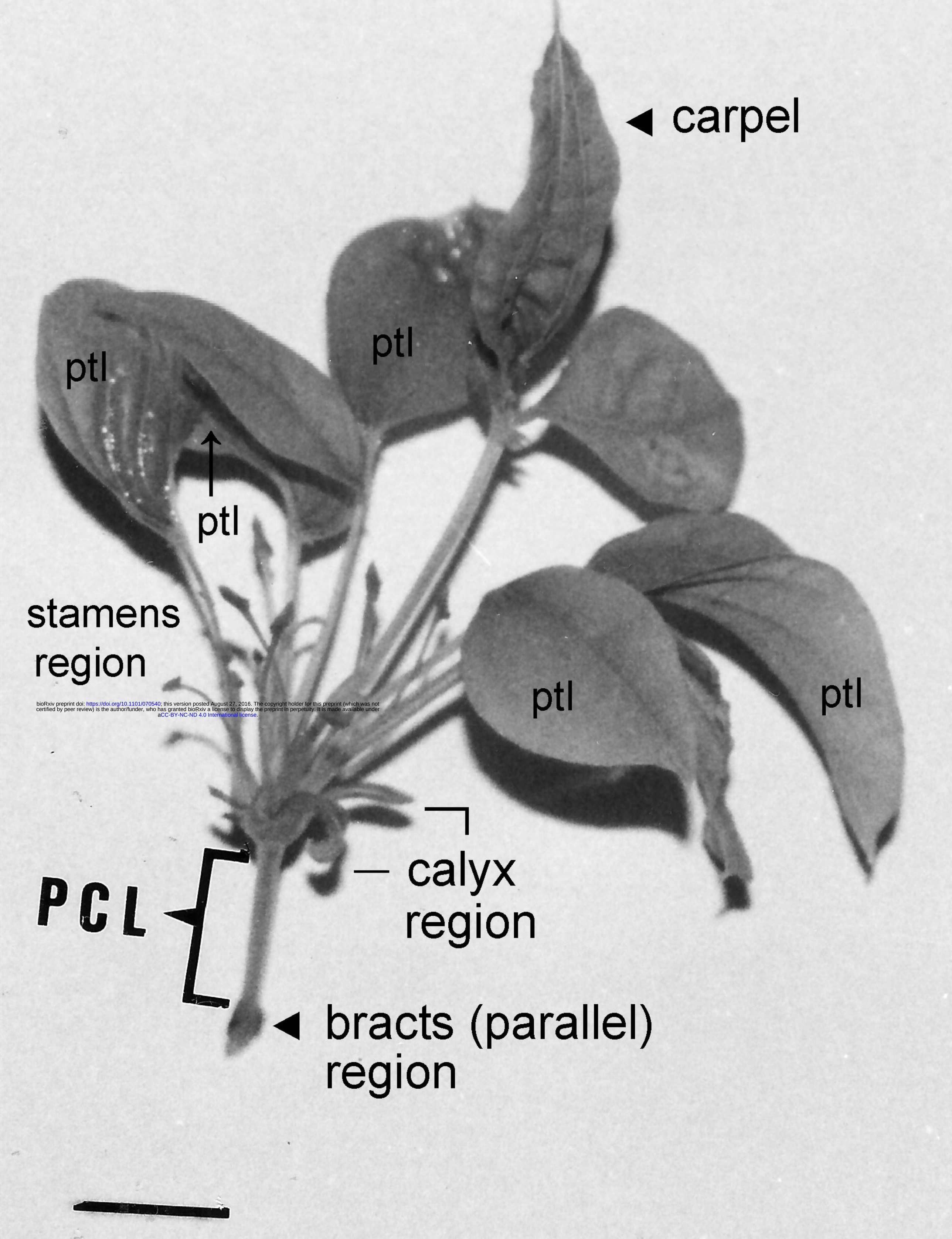

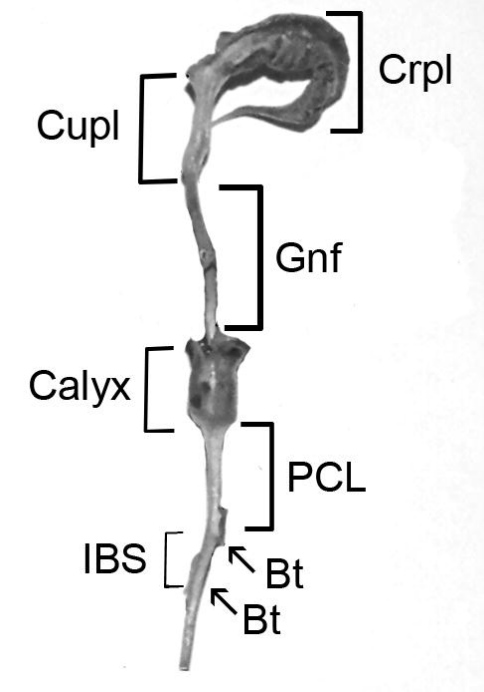
Crpl
Cupl
Gnf
Calyx
PCL
IBS
Bt
Bt

**Table 1:** Putative "necessary structural permutation and developmental steps" within the carpel, begin with ground state, un-webbed, parallel carpel clefts and progress in steps, each of which can be terminal OR continuous to the next step.

| Step 1 | Step 2 | Step3 | Step 4 | Step 5 | Number of specimens |
|---|---|---|---|---|---|
| 1. Ground state, **carpel un-webbed** (clefts parallel) | | | | | 3 |
| 2. Ground state, carpel un-webbed ⇨ **webbed carpel** (planation) (Fig 4) | | | | | 2 |
| 3. Ground state, carpel un-webbed ⇨ carpel webbed ⇨ **carpel vascularized** (Fig 3) | | | | | 10 |
| 4. Ground state, carpel un-webbed ⇨ carpel webbed ⇨ carpel vascularized⇨ **carpel diadnation** (Fig 5) | | | | | 2 |
| 5. Ground state, carpel un-webbed ⇨ carpel webbed ⇨ carpel vascularized⇨ carpel diadnation⇨ **carpel foliation** (Fig 6) | | | | | 21 |